



PROCEEDINGS OF THE 11th WORLD RABBIT CONGRESS

Qingdao (China) - June 15-18, 2016

ISSN 2308-1910

Session Pathology and Hygiene

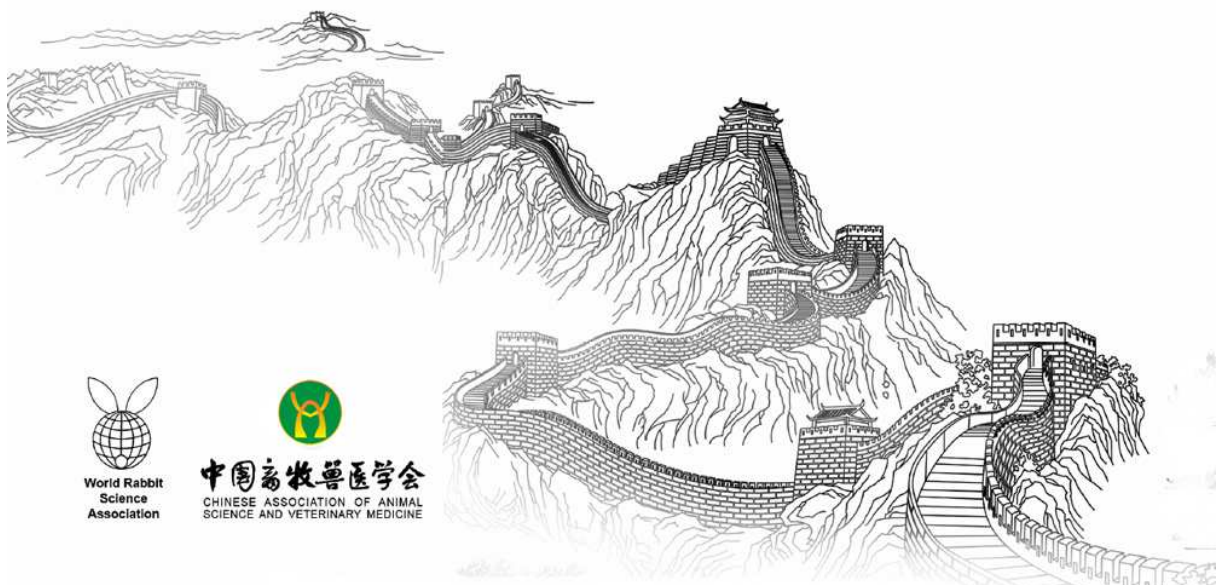
**Song Y.H, Wang F., Fan Z.Y, Hu B., Liu X.,
Wei H.J, Xue J.B., Qiu R.L.**

INTERACTION OF NOVEL RHDV B-CELL EPITOPES WITH HBGA.

Full text of the communication

How to cite this paper :

Song Y.H, Wang F., Fan Z.Y, Hu B., Liu X., Wei H.J, Xue J.B., Qiu R.L. (China) - Interaction of novel RHDV B-cell epitopes with HBGA. *Proceedings 11th World Rabbit Congress - June 15-18, 2016 - Qingdao - China, 627-630.*



INTERACTION OF NOVEL RABBIT HAEMORRHAGIC DISEASE VIRUS B-CELL EPITOPES WITH HISTO-BLOOD GROUP ANTIGENS

Song Yanhua, Wang Fang *, Fan Zhiyu, Hu Bo, Liu Xing, Wei Houjun, Xue Jiabin, Qiu Rulong

Institute of Veterinary Medicine, Jiangsu Academy of Agricultural Sciences · Key Laboratory of Veterinary Biological Engineering and Technology, Nanjing 210014 China - * corresponding author

ABSTRACT

Rabbit haemorrhagic disease (RHD) is caused by the rabbit haemorrhagic disease virus (RHDV). Nine MAbs against VP60 were screened and identified. To map antigenic epitopes, a set of partially overlapping and consecutive truncated proteins spanning VP60 were expressed. The minimal determinants of the linear B cell epitopes of VP60 in the P domain, N³²⁶PISQV³³¹, D³³⁸MSFV³⁴² and K⁵⁶²STLVFN⁵⁶⁹, were recognized by one (5H3), four (1B8, 3D11, 4C2 and 4G2) and four MAbs (1D4, 3F7, 5G2 and 6B2), respectively. Sequence alignment showed epitope D³³⁸MSFV³⁴² was conserved among all RHDV isolates. Epitopes N³²⁶PISQV³³¹ and K⁵⁶²STLVFN⁵⁶⁹ were highly conserved among RHDV G1-G6 and variable in RHDV2 strains. Previous studies demonstrated native viral particles and virus-like particles (VLP) of RHDV specifically bound to synthetic blood group H type 2 oligosaccharides. We established an oligosaccharide-based assay to analyse the binding of VP60 and epitopes to histo-blood group antigens (HBGA). Results showed VP60 and its epitopes (aa 326–331 and 338–342) in the P2 subdomain could significantly bind to blood group H type 2. Furthermore, MAbs 1B8 and 1D4 could block RHDV VLP binding to synthetic H type 2. Collectively, these two epitopes might play a key role in the antigenic structure of VP60 and interaction of RHDV and HBGA.

Keywords: Rabbit haemorrhagic disease virus; VP60 protein; monoclonal antibody; Epitopes; HBGA binding sites

INTRODUCTION

Rabbit haemorrhagic disease virus (RHDV) is the causative agent of rabbit haemorrhagic disease (RHD). The main target of the host immune defence against RHDV is the capsid protein VP60 which is composed of the N-terminal arm (NTA), the shell (S), and the protruding (P) domains. The latter consists of sub-domains P1 and P2 (Wang *et al.*, 2013). The subdomain P2, located at the most exposed region of the capsid, is recognized and targeted by host antibodies (Barcena *et al.*, 2004), and might also contain determinants for cell attachment and antigenic diversity of RHDV. The antigenicity of the VP60 protein has also been reported by other research groups (Laurent *et al.*, 2002). Histo-blood group antigens (HBGA), which act as attachment factors for RHDV, are important for virus infection and might initiate the viral replication cycle (Nystrom *et al.*, 2011). Native viral particles of RHDV as well as virus-like particles isolated from recombinant viral capsid proteins specifically bound to synthetic B, A and H type 2 blood group oligosaccharides (Nystrom *et al.*, 2011). Multiple studies have identified specific residues within the norovirus P2 subdomain that are important for antibody and HBGA interactions (Debbink *et al.*, 2012). Unfortunately, the relationship between antibody and HBGA in RHDV remains unclear.

MATERIALS AND METHODS

Virus and cells

The wild type derivative (rAc-WT) of *Autographa californica* nuclear polyhedrosis virus (ApNPV) and the recombinant AcNPV (rAc-VP60) containing the RHDV VP60 gene (WF-China-2007: FJ794180) were stored in our laboratory (Chen *et al.*, 2014).

Preparation, identification of MAbs and precise localization of epitopes

The RHDV particles (VLPs) were expressed and purified according to previously described methods (Chen *et al.*, 2014). MAbs were screened according to a standard hybridoma technique (Chaithirayanon *et al.*, 2002). The purified VLPs and the native RHDV reacted with MAbs by Western blot and indirect immunofluorescence assay (IFA). A series of primers were designed and synthesized to amplify the truncated fragments of VP60.

Alignment of epitope sequences

The amino acid sequences of VP60 were downloaded from GenBank. Multiple alignments of amino acid sequences of epitopes were created using DNASTAR MegAlign software.

Binding assay of the VLPs and truncated VP60 proteins on synthetic carbohydrates

The synthetic carbohydrate-binding assays were performed as previously described (Nystrom *et al.*, 2011; Uusi-Kerttula *et al.*, 2014). The polyacrylamide (PAA)-biotin conjugated H type 2 trisaccharides (5 µg/ml; GlycoTech, Gaithersburg, MD) were coated on a Pierce® NeutrAvidin® High Binding Capacity Coated 96-Well Plate (Thermo, USA) overnight at 4°C. After blocking, VLPs, made of VP60 (VP60 VLPs), at 0.25–4.0 µg/mL in PBS were used to detect VP60 VLPs binding to synthetic carbohydrates and incubated for 1 h at 4°C. The bound VLPs were then detected with MAb 1B8 (at dilution of 1:1000). The truncated proteins were added at a concentration of 2 µg/ml in PBS. The truncated proteins S1, S3 and S8 were detected by MAbs 1B8; and the truncated proteins F1, F3 and F8 were detected by MAb 1D4 and the truncated proteins C1, C7 and C8 were detected by MAb 5H3 (all diluted at 1:1000). Next, horseradish peroxidase (HRP) conjugated goat anti-mouse IgG antibodies were added for 1 h at 37°C. The enzyme signals were detected at 450nm in an automatic ELISA plate reader. Sf9 cells infected with rAc-WT and PBS were used as controls that received the same treatment as did the VP60 VLPs.

RHDV MAbs blocking of HBGA binding to VLPs and the truncated VP60 proteins

The ability of the MAbs to block the binding of VLPs and the truncated VP60 proteins to H type 2 carbohydrates was tested using specific MAbs (1:1000). RHDV VLPs and the truncated VP60 proteins were pre-incubated with specific MAbs for 1 h at 37°C before transfer to the oligosaccharide-coated plate. Ascites of mice inoculated with SP2/0 myeloma cells and PBS were used as a negative control and a blank control, respectively. The VLPs and the truncated VP60 proteins (in the presence or absence of MAb) were added to carbohydrate-coated plates and incubated for 2 h. After washing, MAbs at a dilution of 1:1000 were added into corresponding wells, followed by incubation with HRP-conjugated goat anti-mouse IgG. The levels (%) of blocking were calculated from the difference in OD450 values between wells with pre-incubation with MAbs or ascites of mice inoculated with SP2/0 myeloma cells.

Statistics

Statistical significance was determined using one-way repeated measurement ANOVA and least significance difference (LSD) test.

RESULTS AND DISCUSSION

Preparation and identification of MABs

Electron microscopy analysis showed expressed VP60 self-assembling into VLPs. We obtained nine MABs and identified as 1B8, 1D4, 3D11, 3F7, 4C2, 4G2, 5G2, 5H3, and 6B2. All MABs recognized RHDV VLPs and native RHDV by Western blot analysis and IFA.

Precise localization of epitopes and alignment of epitope sequences

Precise localization of epitopes were detailed and reported by Song *et al.*, (2016).

We aligned the epitope sequences among 21 RHDV strains encompassing RHDV genogroups 1–6 as well as the RHDV2 (RHDVb) variant, to investigate conservation of the epitopes. The epitope D³³⁸MSFV³⁴², recognized by MAb 1B8, 3D11, 4C2 and 4G2, was completely conserved among all the RHDV isolates (Figure. 1). The epitope N³²⁶PISQV³³¹, recognized by 5H3, was highly conserved among all RHDV strains, except for a V331→I331 substitution in RHDV2 strains (Figure 1). The K⁵⁶²STLVFNL⁵⁶⁹ epitope, recognized by 1D4, 3F7, 5G2 and 6B2, was relatively conserved among the RHDV G1–G6 strains, but it was variable in RHDV2 strains with K562→T562 and F567→Y567 (Figure 1).

		326aa	331aa	338aa	342aa	562aa	569aa
G6	WF-China-2007	N	P	I	S	Q	V
	AST89
G1	Eisenhuettenstadt
	France 00-08
	Mexico99
G2	Narrawa 2006
	New Zealand
	France 05-01
	Frankfurt
G3-5	Hagenow
	Meiningen
	Rainham
	Wriezen
	France 03-24
G6	Iowa2000
	Isolate SH China 2006
	XA-China-2010
	Strain 10-01
	strain 10-07
	strain 10-28
RHDVb	Ud11

Binding of VLPs and truncated VP60 proteins to HBGA

When VP60 VLPs were titrated for binding to oligosaccharide by ELISA, a linear relationship between binding and VLP concentration was observed between 0.25–4.0 µg/mL (Figure. 2(a)). The truncated proteins C1, C7, and C8 could specifically react with the PAA-biotin conjugated H type 2 trisaccharides (Figure.2 (b)) as detected by MAb 5H3. Compared with the control group, the reaction values of C1, C7, and C8 had statistical significance ($p < 0.01$). Similar results

Figure 1 Alignment of epitope sequences of VP60 among 21 RHDV G1-G6 and RHDVb strains

were found for the truncated proteins S1, S3, and S8 detected by MAb 1B8 ($p < 0.01$) (Figure 2(c)). However, the OD values measured for binding to truncated proteins F1, F3 and F8 did not significantly differ from those of the PBS group ($p > 0.05$) (Figure 2(d)). Hence, F1, F3 and F8 did not react with HBGA. The OD values measured for the VP60 positive control revealed significant differences when compared to PBS ($p < 0.01$) (Figure 2(b, c, d)).

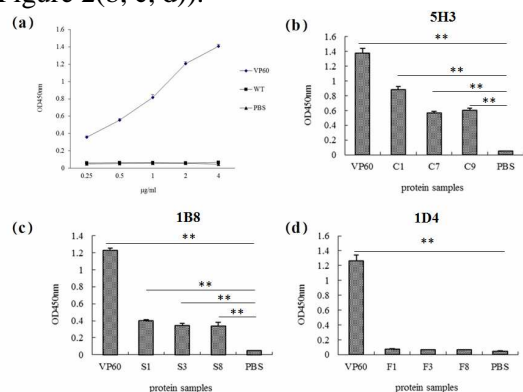


Figure.2 RHDV VP60 VLPs binding to synthetic oligosaccharides and synthetic oligosaccharide binding of the truncated proteins. **indicates a significant difference between groups ($p < 0.01$)

RHDV MAB blocking of VLP and truncated VP60 protein binding to HBGA

Blocking activity was scored based on levels of reduction of the OD values in wells with or without blocking MABs. The OD values of wells containing blocking MABs significantly differed from those of the negative control group without MABs ($p < 0.01$) (Figure 3(a, c)). MAb 5H3 could strongly block binding of truncated proteins C1, C7 and C8 to oligosaccharide conjugates with a blocking rate of almost 100% (Figure 3(a, b)). Furthermore, this MAB partially blocked the binding of the VP60 VLPs to oligosaccharide conjugates by ~70% (Figure 3(b)).

Likewise, MAb 1B8 could also completely block S1, S3 and S8 binding to oligosaccharide conjugates (Figure 3(c, d)). It only blocked ~50% of the binding of the VP60 VLPs to oligosaccharide (Figure 3(d)).

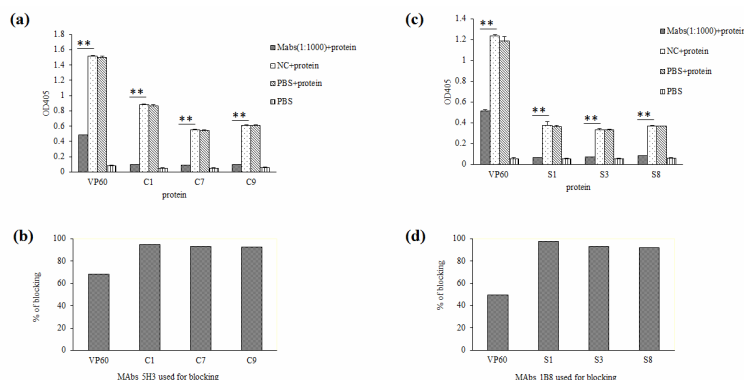


Figure 3 Blocking of VP60 VLPs and truncated protein binding to synthetic oligosaccharides. **indicates a significant difference between groups ($p < 0.01$).

CONCLUSIONS

These new findings extend our understanding of RHDV–HBGA interactions and help to elucidate the relationship between antigenicity and HBGA binding sites in RHDV infections.

ACKNOWLEDGEMENTS

The project was supported by the National Natural Sciences Foundation of China (31502073), the Jiangsu Province Natural Sciences Foundation (BK20140740) and the earmarked fund for China Agriculture Research System (No. [CARS-44-C-1]).

REFERENCES

Barcena, J., Verdager, N., Roca, R., Morales, M., Angulo, I., Risco, C., Carrascosa, J. L., Torres, J. M. & Caston, J. R. 2004. The coat protein of Rabbit hemorrhagic disease virus contains a molecular switch at the N-terminal region facing the inner surface of the capsid. *Virology*, 322, 118-134.

Chaithirayanon, K., Wanichanon, C., Vichasri-Grams, S., Ardeungneon, P., Grams, R., Viyanant, V., Upatham, E. S. & Sobhon, P. 2002. Production and characterization of a monoclonal antibody against 28.5 kDa tegument antigen of *Fasciola gigantica*. *Acta Trop*, 84, 1-8.

Chen, M., Song, Y., Fan, Z., Jiang, P., Hu, B., Xue, J., Wei, H. & Wang, F. 2014. Immunogenicity of different recombinant rabbit hemorrhagic disease virus-like particles carrying CD8+ T cell epitope from chicken ovalbumin (OVA). *Virus Res*, 183, 15-22.

Debbink, K., Donaldson, E. F., Lindesmith, L. C. & Baric, R. S. 2012. Genetic mapping of a highly variable norovirus GII.4 blockade epitope: potential role in escape from human herd immunity. *J Virol* 86, 1214-1226.

Laurent, S., Kut, E., Remy-Delaunay, S. & Rasschaert, D. 2002. Folding of the rabbit hemorrhagic disease virus capsid protein and delineation of N-terminal domains dispensable for assembly. *Arch Virol* 147, 1559-1571.

Nystrom, K., Le Gall-Recule, G., Grassi, P., Abrantes, J., Ruvoen-Clouet, N., Le Moullac-Vaidye, B., Lopes, A. M., Esteves, P. J., Strive, T., Marchandeu, S., Dell, A., Haslam, S. M. & Le Pendu, J. 2011. Histo-blood group antigens act as attachment factors of rabbit hemorrhagic disease virus infection in a virus strain-dependent manner. *PLoS Pathog*, 7, e1002188.

Song Y, Wang F*, Fan Z, Hu B, Liu X, Wei H, Xue J, Xu W, Qiu R. 2015. Identification of novel rabbit haemorrhagic disease virus B-cell epitopes and their interaction with host histo-blood group antigens. [J]. *J. Gen. Virol.*, 97:356-365.

Uusi-Kerttula, H., Tamminen, K., Malm, M., Vesikari, T. & Blazevic, V. (2014). Comparison of human saliva and synthetic histo-blood group antigens usage as ligands in norovirus-like particle binding and blocking assays. *Microbes Infect*. 16, 472-480.

Wang, X., Xu, F., Liu, J., Gao, B., Liu, Y., Zhai, Y., Ma, J., Zhang, K., Baker, T. S., Schulten, K., Zheng, D., Pang, H. & Sun, F. (2013). Atomic model of rabbit hemorrhagic disease virus by cryo-electron microscopy and crystallography. *PLoS Pathog*, 9, e1003132.